Bulletin of Geography – Physical Geography Series
No 6/2013: 7–25 http://dx.doi.org/10.2478/bgeo-2013-0001

DMITRY Yu. DEMEZHKO[1],
ANASTASIA A. GORNOSTAEVA[1],
GEORGY V. TARKHANOV[2], OLEG A. ESIPKO[2]

[1]Institute of Geophysics UB RAS, 100 Amundsen Str., 620016,
Yekaterinburg, Russia
ddem54@inbox.ru
[2]JSC "SIC Nedra", 8/38 Svobody Str., 150000, Yaroslavl, Russia

30,000 YEARS OF GROUND SURFACE TEMPERATURE AND HEAT FLUX CHANGES IN KARELIA RECONSTRUCTED FROM BOREHOLE TEMPERATURE DATA

Abstract: Analyses of temperature-depth profiles logged in deep boreholes (> 1 km) permit the reconstruction of ground surface temperature (GST) and surface heat flux (SHF) histories in the period of global climate change at the border of the Pleistocene and the Holocene. We reconstructed past GST and SHF histories using data obtained from the 3.5-km-deep Onega borehole (Karelia, north-west Russia). The resulting reconstructions include information on the basal thermal regime of the Scandinavian Ice Sheet, which covered the region in the Last Glacial Maximum (LGM). The surface temperature history reveals a high amplitude of Pleistocene/Holocene warming equal to 18–20 K. The heat flux changes precede the surface temperature changes and are close to the variations of insolation at a latitude of 60°N. A comparison of the reconstructed GST and SHF histories with the records of carbon dioxide contents in Antarctic ice cores shows that CO_2 changes are much closer to temperature changes than they are to heat flux changes.

Key words: Borehole temperatures, paleoclimate reconstruction, Pleistocene/Holocene transition, surface temperature, heat flux, Karelia

Introduction

The vertical distribution of today's ground temperatures contains important information relevant to past climatic changes in ground surface temperature and heat flux through the surface. Thermal anomalies occurring due to climate change slowly permeate downwards and disturb steady-state thermal fields. The depth of penetration of thermal anomalies is determined by the time elapsed after climate change and the thermal properties of the rock. Thus, diurnal variations do not penetrate below 0.5–1 m, while annual variations penetrate 20–30 m and secular temperature variations are registered within a few hundred meters, and the impact of global warming in the early Holocene (about 10 kyr ago) is traced to a depth of 1.5–2 km. The climatic signal persists in the form of anomalous ground temperature distributions over a period comparable to the period of surface temperature variations (Demezhko 2001). Analyzing present temperature distributions in boreholes, one can evaluate ground surface temperature histories (GSTH) and surface heat flux histories (SHFH). The first efforts to reconstruct paleotemperatures were made by Hotchkiss and Ingersoll (1934), Birch (1948), Beck and Judge (1969), Cermak (1971), Beck (1982), Lachenbruch and Marshall (1986). To date, several thousands of GSTH reconstructions have been made all over the world (see: Bodri and Cermak 2007 and reference therein). Most of them are limited to recent centuries, while some hundreds of them comprise the last millenium, while at most only twenty reconstructions dip into the past by up to tens of thousands of years (Bodri and Cermak 1997; Rajver et al. 1998; Dahl-Jensen et al. 1998; Demezhko and Shchapov 2001; Demezhko et al. 2007; Golovanova et al. 2012).

Little attention has been given to the use of geothermal data to estimate energy balance variation at the Earth's surface. Majorowicz et al. (2012a) have calculated subsurface temperatures from solar-induced climatic forcing in Western Canada over the period from 1986 to 2006 using information about climate sensitivity. The comparison of these evaluated temperature-depth profiles with repeated well-log data has shown that less than one third of the observed anomalies can be explained by solar forcing. Direct reconstructions of SHFHs were carried out in timescales from several centuries to a millenium (Wang and Bras 1999; Beltrami et al. 2002, 2006; Huang 2006). At the same time, the reconstructions of long-term surface heat flux variations are of importance in order to understand the energy

of climatic processes. This information may be useful for the verification of general circulation models (GCMs). Since the reconstructed heat flux is the difference between large values (those of net radiation, sensible and latent heat fluxes – Anderson et al. 2011), it is difficult to measure its magnitude accurately from meteorological data.

In this work we analyze the temperature data logged in the Onega parametric borehole, which is situated in Karelia, north-west Russia. The borehole depth permits the reconstruction of GSTH and SHFH for the last 30,000 years. This period is of special importance for understanding the Earth's climatic history because about 10,000 years ago the Weichselian glacial period of the Pleistocene ended and the Holocene interglacial began. The study region is also interesting because in the Last Glacial Maximum (LGM) period it was covered by the Scandinavian Ice Sheet. For this reason, the obtained reconstructions include information on the basal thermal regime of the ice sheet.

Physical background

In this study, the reconstruction of GSTH was made using the solutions of the equation for heat in a homogeneous medium without internal heat sources or vertical ground water flow over the observation interval (Carslaw and Jaeger 1959):

$$\frac{\partial^2 T}{\partial z^2} - \frac{1}{a}\frac{\partial T}{\partial t} = 0, \tag{1}$$

with boundary conditions:

$$T(0,t) = T_s(t), \tag{2}$$

$$\left.\frac{\partial T}{\partial z}\right|_{z\to\infty} = G_0, \tag{3}$$

where T is temperature, z is depth, t is time, a is thermal diffusivity, G_0 is the initial undisturbed temperature gradient and T_s is surface temperature. The solution of Eq. (1) can be expressed as a sum:

$$T(z,t) = T_0 + G_0 z + \Theta(z,t), \tag{4}$$

where T_0 is the initial undisturbed surface temperature, Θ is a non-stationary temperature anomaly that appears at the moment $t = t_0$ and satisfies the condition at infinity:

$$\Theta(z,t) = 0,\ z \to \infty \tag{5}$$

A surface temperature history can be taken in the form of a series of m instantaneous surface temperature changes:

$$T_s(t) = \begin{vmatrix} T_0, t < t_1 \\ T_i, t_i < t < t_{i+1} \\ \ldots\ldots\ldots\ldots \\ T_m, t_m < t < t_* \end{vmatrix}. \tag{6}$$

In this case the solution of Eq. (1) is written as follows:

$$\begin{aligned} &T(z,t_*) = T_0 + G_0 z + \sum_{k=1}^{m} D_k erfc(z/L_k), \quad L_k = 2\sqrt{at_k}, \\ &D_k = T_k - T_{k-1},\ t_k = t_* - t_i,\ i,k = 1,2,3,...,m. \end{aligned} \tag{7}$$

Here $erfc(u)$ is the complementary error function and t_* is the time of temperature logging.

For the GSTH reconstruction we used the inversion technique based on a selection of multi-step temperature history which more closely corresponds to the measured temperature-depth profile (in L^2 – metrics). Solution stability was provided by the increase of time intervals into the past in accordance with the resolution power (Demezhko and Shchapov 2001). Then a set of multi-step temperature histories with a different number of time intervals was averaged and smoothed.

As a surface boundary condition, one can also take the heat flux, which is related to the temperature gradient as follows:

$$q(0,t) = -\lambda \left.\frac{\partial T(z,t)}{\partial z}\right|_{z=0}, \tag{8}$$

where λ is thermal conductivity. The solutions of Eq. (1) with the boundary conditions (2, 3, 8) are known (Carslaw and Jaeger 1959). But for evaluating SHFH, it is convenient to directly use the reconstructed GSTH. The relationship between the GSTH (represented by a piecewise linear function of temperature over uniform time intervals Δt), and the SHFH (defined by its constant values within each time interval Δt) (Beltrami 2002; Huang 2006), is as follows:

$$q(0,t_i) = \frac{2e}{\sqrt{\pi \Delta t}} \sum_{j=1}^{i} \left[T_{j-1} - T_j\right] \cdot \left[\sqrt{i-(j-1)} - \sqrt{i-j}\right], \qquad (9)$$

where e is thermal effusivity defined as $e = (\lambda \cdot \rho C)^{1/2} = \lambda / \cdot (a)^{1/2} = \rho C (a)^{1/2}$.

Geothermal data

The Onega parametric borehole (62.1°N, 34.5°E) was drilled by JSC SIC "Nedra" on December 31, 2008 to a depth of 3,500 m in the northwest part of the Palaeoproterozoic Onega structure. The 2,944-m-thick volcanic sedimentary succession rests on an Archean granite-greenstone basement (Fig. 1). The lowermost part of this succession (2,115–2,944 m, the Jatulian super-horizon), includes a 194-m-thick halite-anhydrite bed which lies directly on the basement (Glushanin et al. 2011).

A geothermal survey was performed by JSC SIC Nedra. A total of 9 temperature loggings were conducted, both in the process of drilling and after its completion. For the temperature history reconstruction we chose the temperature-depth profile logged at a depth of 2,523 m on the 3rd of July 2008, after a two-month break in drilling resulting from drilling problems (Fig. 2, curve 1). More recent and deeper temperature records (the 30th of August 2008 and the 2nd of February 2009) were obtained after the borehole passed the halite-anhydrite bed. These profiles clearly manifest a negative temperature anomaly related to the thermal effect of salt dissolving. The temperature gradient calculated from T(z) profile (Fig. 2, curve 2) traces the periodic components which may be related to the rhythmicity of volcanic processes and the corresponding changes in the rock's thermal properties. The amplitude spectrum of the temperature gradient variations shows a predominance of rhythms with wavelength of 20–80 m and 140–300

m (Fig. 3). This specifically geological feature may be wrongly attributed to the ground surface temperature change with a period of τ:

$$\tau = \frac{L^2}{4\pi a}, \qquad (10)$$

where L is a temperature wavelength in the borehole. If L = 300 m, $a = 10^{-6}$ m^2 per sec we obtain τ = 230 years. Since the temperature field $T(z)$ remains a "trace" of only one (the last) period of any surface temperature fluctuations $T(t)$, in order to avoid the appearance of a spurious episode

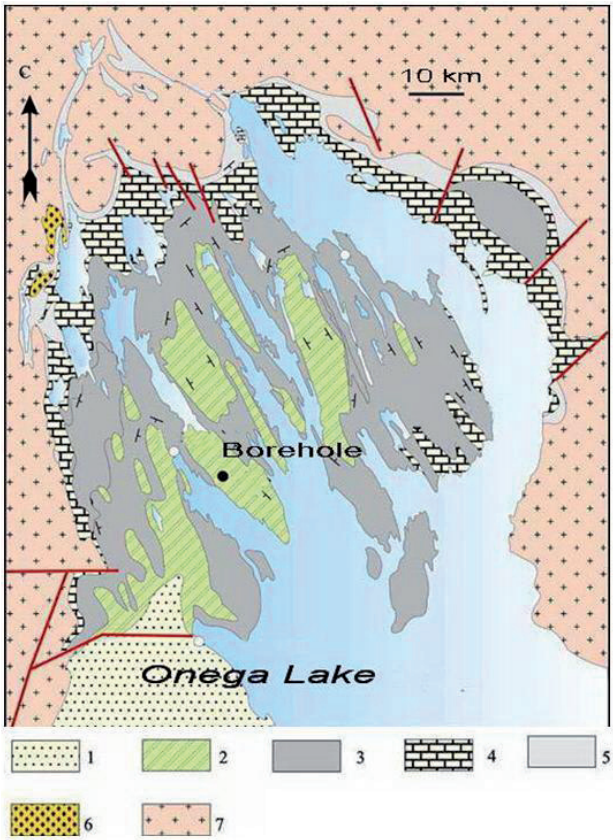

Fig.1. Simplified geological map of the study area (Narkisova 2009). 1 – Vepsian super-horizon; 2 – Kalevian super-horizon; 3 – Ludicovian super-horizon; 4,5 – Jatulian super-horizon; 6 – Sariolian super-horizon; 7 – Archean basement

of climatic history it makes sense to eliminate the upper part of the $T(z)$ profile from the inversion. Therefore, we excluded the upper 400 m of the temperature log from our analysis. At its lower part, the $T(z)$ profile was limited to a depth of 2,200 m. Below this limit the variation of temperature gradient sharply increases due to the replacement of Ludicovian volcano sedimentary succession by a Jatulian sedimentary formation including the thick halite-anhydrite bed (Glushanin et al. 2011).

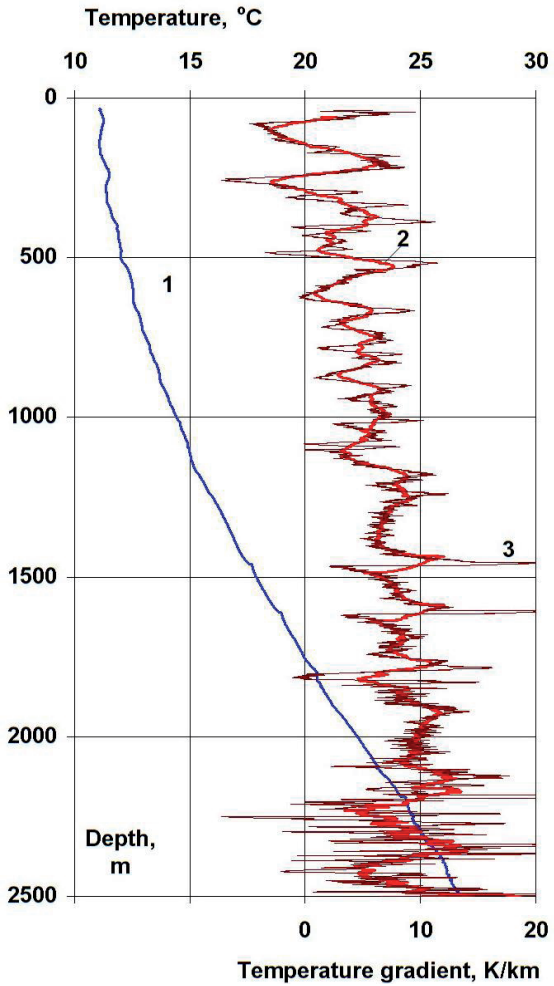

Fig. 2. The change of temperature (1) and temperature gradient, smoothed in 50-m (2) and 10-m (3) running windows

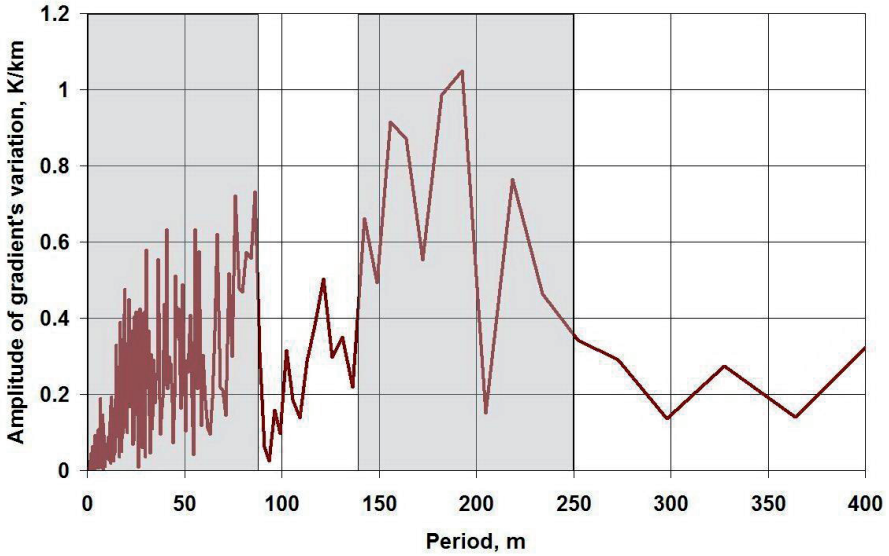

Fig. 3. The amplitude spectrum of temperature gradient variations

GSTH reconstruction and its correction

The reconstruction of GSTH using the data obtained by temperature logging in the Onega parametric borehole (interval 400–2,200 m) is shown in Figure 4. The temperature history was approximated by *m*-step function with a progressively increasing number of steps. The initial thermal diffusivity value was assumed to be $a = 1.0 \cdot 10^{-6}$ m^2 per sec. Temperature histories with $m = 7, 8, 9, \ldots 13$ represent an ensemble of equivalent temperature histories. The result of their averaging and smoothing is shown in Figure 4 (the solid curve); the thin curves bordering it show a range of two standard deviations.

Although the reconstructed history reproduces the main climatic event on the border of Pleistocene and Holocene, i.e. the warming by 12 K from 15 to 9 kyr ago, it requires further correction in order to take into account the insufficient restoration of thermal equilibrium after the completion of drilling, as well as the possible departure of the thermal diffusivity from its accepted value. The borehole temperature at the top of the temperature record (30 m) is 11.1°C. This is significantly higher than the mean annual soil temperature in the region and points to insufficient restoration of the thermal regime. It has been shown (Demezhko and Shchapov 2001) that

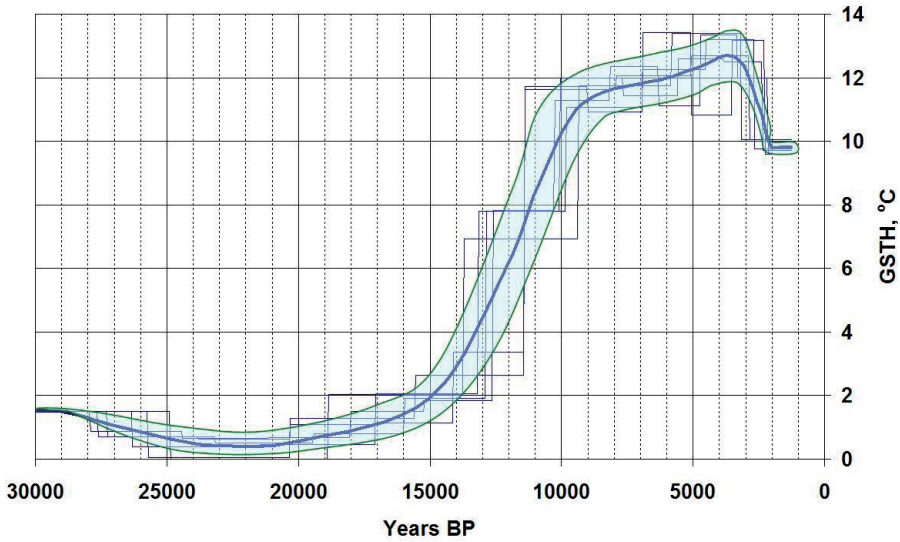

Fig. 4. GSTH reconstruction (when a = $1.0 \cdot 10^{-6}$ m^2 per sec). Polylines are the assemblage of equivalent histories, a solid blue line is the result of their averaging and smoothing, and green lines delimit the range of «the average ± standard deviation».

the amplitude of paleotemperature oscillations reconstructed from such temperature-depth profiles is underestimated. The distortion degree may be evaluated by the factor F:

$$F = \frac{T_s - T_s^u}{\breve{T} - T_s^u}, \qquad (11)$$

where T_s, T_s^u are, respectively, the measured and the undisturbed values of long-term average ground surface temperature, while $\breve{T}$ is the average temperature in the borehole. The real amplitude will be $k = 1/(1 - F)$ times higher than the reconstructed amplitude.

According to (Sonin 2001) the soil temperature at the depth where annual temperature fluctuation is almost completely attenuated (15–20 m) is about 5.2–5.5°C for the study area. Close values of annual soil temperature 5.3–6.1°C were recorded in the nearest regions of Finland (Maaninka and Tohmajarvi) (Yli-Halla and Mokma 1998). The calculation results of the

factor F and the correction coefficient k for two extreme values of the mean annual soil temperature are presented in Table 1.

Table 1. The F and k values

T_s, °C	T_s^u, °C	$\check{T}$(30-2523 m), °C	F	k=1/(1- F)
11.1	5.2	17.2	0.49	1.97
	6.1		0.45	1.82

As seen from this table it is necessary to almost double the amplitude of reconstructed paleotemperatures. The corrected temperature history may be calculated by-

$$T_s^{corr}(t) = T_s^u + k[T_s\ (t) - T_s^u]. \qquad (12)$$

While insufficient restoration of the temperature regime after drilling decreases the amplitude of the reconstructed temperature changes, the difference between accepted thermal diffusivity and its true value leads to time-scale bias. Without setting *a priori* the value of this coefficient we can reconstruct the temperature history in coordinates [T_s, at_*], where a is thermal diffusivity, and t_* is the time from the climatic event to the moment of logging. So, if the accepted thermal diffusivity is p-times higher than the real one, then for correction of GSTH it is necessary to also stretch it out p-times over the time scale.

Information about the thermal diffusivity of volcano-sedimentary rocks is extremely poor. For the Quaternary volcano-sedimentary rocks from Kunashir Island we have obtained the estimation of a equal to $0.7 \cdot 10^{-6}$ m^2 per sec (Demezhko and Solomina 2009). One can assume that the thermal diffusivity of palaeoproterosoic volcano-sedimentary rocks is slightly above this estimate. Let's take it as equal to $a = 0.75 \cdot 10^{-6}$ m^2 per sec. The GSTH corresponding to this estimate is shifted to an earlier time by 25% (curve 3 in Fig. 5).

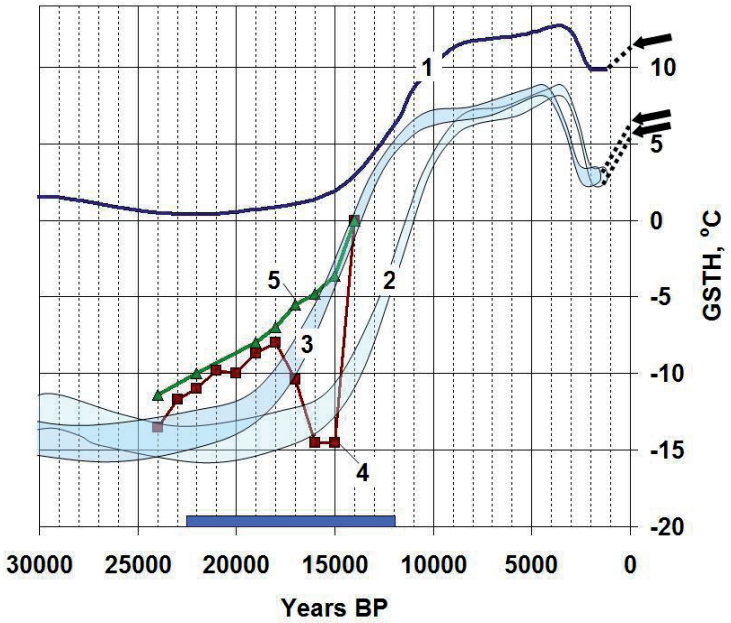

Fig. 5. Correction of GSTH. 1 – The initial reconstruction (with a = $1.0 \cdot 10^{-6}$ m^2 per sec). 2 – correction for the influence of insufficient thermal regime restoration. The filled area between the curves (2) corresponds to the uncertainty of T_s^u value (T_s^u = (5.2–6.1)°C). The filled area (3) is the same with a = $0.75 \cdot 10^{-6}$ m^2 per sec. Curves 4 and 5 are the results of temperature simulation in the base of the Scandinavian Ice Sheet for Karelia (4) and the Otokumpu local area (5) (Forsström 2005). The glaciation interval of Onega lake is marked by the blue bar (Lunkka et al. 2001; Saarnisto and Saarinen 2001)

SHFH evaluation

The surface heat flux history (SHFH – Fig. 6, brown curve) was calculated from the corrected GSTH (curve 3 in Fig. 5) using Eq. 9. The following values of thermophysical parameters were taken: $a = 0.75 \cdot 10^{-6}$ m^2 per sec, $\lambda = 2.2$ $Wm^{-1}K^{-1}$, $e = 2540$ $J \cdot K^{-1}m^2sec^{-½}$. The SHFH is essentially different from the GSTH. The heat flux changes precede the surface temperature changes (this is clearly seen when comparing the corresponding curves in Figure 7). The heat flux reached its maximum value of 0.11 Wm^{-2} 14.5–12.5 kyr ago and then began to decline. The reconstructed SHFH in the period of 2.5–24 kyr ago is sufficiently close to the curve of annual insolation variations at a latitude of 60° N, which is determined by changes

in the Earth's orbital parameters (Berge and Loutre 1991)—see Figure 6. In addition, the amplitude ratio A_{SHFH}/A_I amounts to 1.2%. For the annual cycle the relation between the soil heat conduction flux and net radiation can vary over a wide range—from 3 to 35% (Choudhury et al. 1987; Anderson et al. 2008; Krapez et al. 2009). It is generally governed by the value of LAI (leaf area index). However our estimation of $A_{SHFH}/A_I = 1.2\%$ is outside this range. It may be suggested that in long-term climate changes a significant role was played by feedbacks which hindered heat propagation to deeper soil layers.

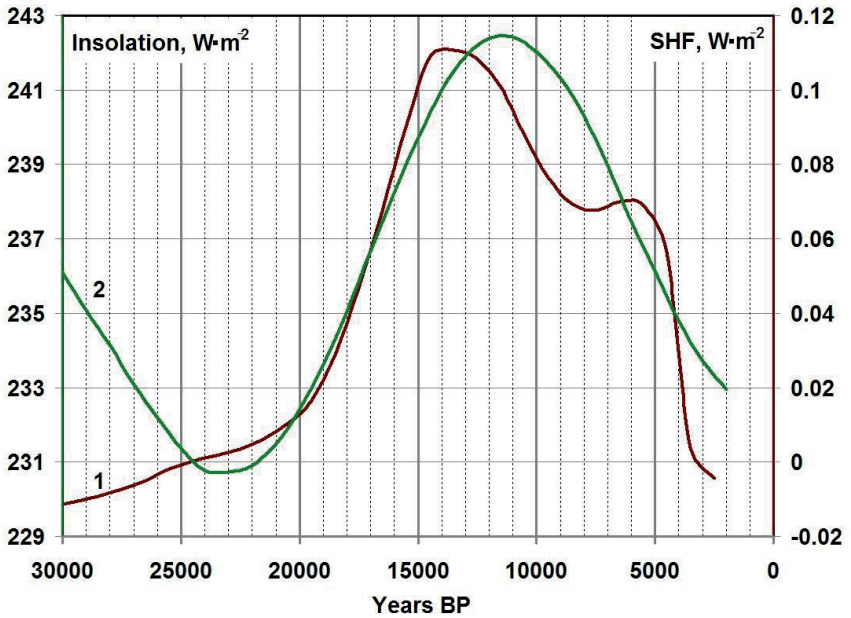

Fig. 6. A comparison of the reconstructed SHFH (1) and insolation (2) at the latitude of 60° N, which is determined by changes in the Earth's orbital parameters (Berge and Loutre 1991)

Discussion

Temperature profiles of deep boreholes often contain a "heat trace" of paleopermafrost. The latent heat of ice thawing must usually be taken into account in these cases. It is especially important for boreholes drilled in porous sedimentary rocks (Šafanda et al. 2004; Majorowicz et al. 2012b). Let us evaluate *ex post facto* the possible distortions which could be made

in the reconstruction when the influence of permafrost is ignored. Volcano-sedimentary rocks of Paleoproterozoic Onega structure have a high density (ρ = 2.7–2.9 g/cm^3) and low porosity (Φ = 0.2–0.5%) (Narkisova 2009). Knowing the mean ground surface temperature during the Late Pleistocene T_0 and the undisturbed geothermal gradient G_0, we can find the permafrost thickness: $h_{perm} = -T_0/G_0$. The ground surface temperature during the period 30–20 kyr BP according to our reconstruction (Fig. 5) was T_0 = -14°C. The undisturbed geothermal gradient G_0 can be estimated by multiplying the measured gradient at the lowermost part of the profile $G_{meas} = 10.7 \cdot 10^{-3}$ K/m (Fig. 2) by a factor of k = 1.9 (Table 1): $G_0 = 10.7 \cdot 10^{-3} \cdot 1.9 = 20.3 \cdot 10^{-3}$ K/m. Hence, $h_{perm} \approx 700$ m. The heat required to completely melt the permafrost can be calculated as: $Q = \rho_i L \Phi h_{perm}$, where $L = 334 \cdot 10^3$ J/kg is the specific heat of ice thawing, and $\rho_i = 1 \cdot 10^3$ km/m^3 is ice density. For Φ- = 0,5% and $h_{perm} \approx 700$ m we'll obtain $Q = 1.2 \cdot 10^9$ J/m^2. For comparison, the total heat absorbed by the ground for a period of anomaly insolation 24–5 kyr BP according to our reconstruction (SHF curve in Fig. 6) is $Q_{abs} = \int \mathrm{SHF}\,(t)\,dt = 3.0 \cdot 10^{10}$ J/m^2. So, only 3.3% of the absorbed heat was spent on the permafrost thawing. This percentage may be even less, since the calculation does not take into account the bound water, the proportion of which may have been significant at such low porosity. We can assume that the permafrost-related error also does not exceed 4%.

The corrected temperature history reveals a suddenly high amplitude of Pleistocene/Holocene warming equal to 18–20 K. This is approximately twice as high as the amplitude reconstructed from the temperature-depth profile logged in the Otokumpu borehole (Kukkonen et al. 2011) and 5.5 times higher than the proxy estimation of average global amplitude (Shakun et al. 2012). At the same time they have a good correlation with a number of different geothermal estimates for the region (Safanda et al. 2004; Kukkonen et al. 1998). According to the empirical model of the spatial distribution of Pleistocene/Holocene warming amplitudes which generalize previously obtained long-term geothermal reconstructions (Demezhko et al. 2007), the warming amplitudes decreased in inverse proportion to the distance from the hypothetical warming center which is situated in the North Atlantic. For the region under study the model gives a warming amplitude estimation of 18 K. The absolute temperature values in the Late Weichsellian agree well with the simulation results of the

Scandinavian Ice Sheet basal thermal regime (Forsström 2005), as shown by curves 4 and 5 in Figure 5.

The synchronous changes of the heat flux and insolation indicate that, in the period of 2.5–24 kyr ago, ground surface temperature changes were mainly governed by external radiative forcing. However, the role of the Scandinavian Ice Sheet in the generation of the ground surface temperature regime in the region remains unclear. The glaciation of the northern part of Onega Lake began approximately 23–22 kyr ago (Lunkka et al. 2001) and deglaciation happened around 12 kyr ago (Saarnisto and Saarinen 2001). Hence, a significant part of the reconstructed warming occurred under the thickness of the ice. To explain the absence of glaciation evidence in the geothermal reconstructions it is necessary to allow for the ambiguous role of the ice sheet in the generation of its basal thermal regime. While the ground surface in the region was ice-free its temperature changed in agreement with surface air temperature changes. Once the glacier had appeared the geothermal heat flow and vertical ice flow came to play a significant role in the thermal regime (Demezhko et al. 2007). The heat flow from the Earth's interior caused the heating at the bottom of glacier, and conversely the vertical flow contributed to its cooling. In addition, glacial bed topography and friction influenced the thermal regime. All of these factors lead to the high spatial variability of temperatures at the base of the ice sheets, as evidenced by the results inferred from deep borehole temperature profiles (Majorowicz 2012). In our case, we can only assume that the influences of these factors compensated for each other, and the glacier's existence only slightly affected ground surface temperature changes.

A comparison of the reconstructed GSTH and SHFH with the records of carbon dioxide contents in the Antarctic ice cores leads to another important conclusion. In general, the data on CO_2 changes during the last deglaciation are related to global and hemispheric temperatures to determine cause-effect relations between these factors (see Shakun et al. 2012 and references therein). If the CO_2 increase leads the temperature increase, then one can infer the existence in the warming mechanism of an additional forcing resulting from the greenhouse effect. Conversely, the precedence of temperatures would point to CO_2 having a passive role in the warming. In our opinion, conclusions based on such arguments are highly unreliable because both carbon dioxide content and air bubble age estimations are

made with a high degree of uncertainty (Fig. 7). For the confirmation of a hypothesis that CO_2 and green-

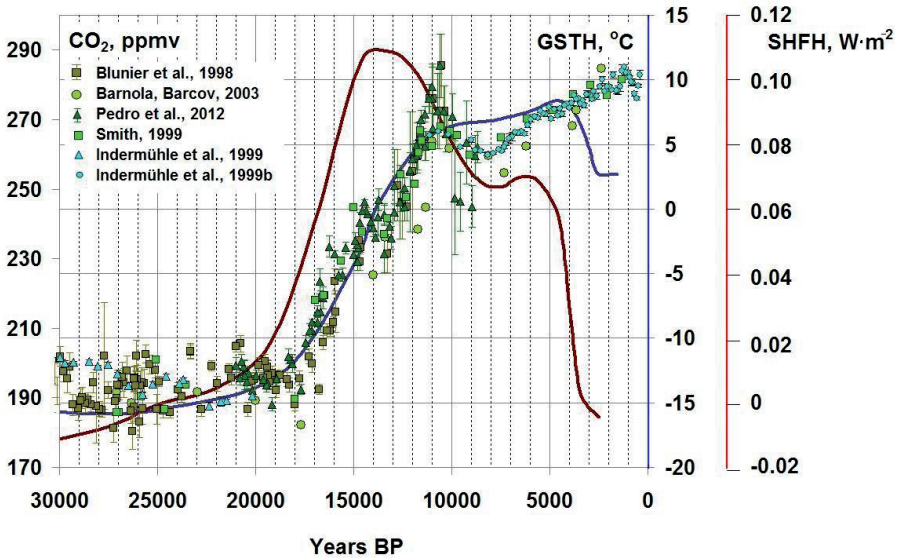

Fig. 7. A comparison of the reconstructed GSTH (blue curve), SHFH (brown curve) and the carbon dioxide contents in the Antarctic ice cores (markers)

house forcing played a significant role in Pleistocene/Holocene warming, it would be logical to compare these data not only with temperatures but also with the reconstructed radiative forcing. The SHFH and GSTH reconstructions and the CO_2 data shown in Figure 7 indicate that changes in carbon dioxide by its shape and chronology are much closer to temperature changes than they are to heat flux changes. The heat flux increase occurred at a faster pace, and then 12 kyr ago it began to fall, while the increase in CO_2 continues to the present. These differences are clearly visible even against the backdrop of uncertainty in the estimates of CO_2. On the assumption that the reconstructed SHFH generally reproduces changes in radiative forcing, one can challenge the hypothesis of the primary role of CO_2 and the greenhouse effect in Pleistocene/Holocene warming.

Acknowledgments

The authors would like to thank two anonymous reviewers for their useful comments, constructive suggestions and improvements of the text. This research was supported by the Russian foundation of fundamental researches (grant 13-05-00724a)

References

ANDERSON M.C., NORMAN J.M., KUSTAS W.P., HOUBORG R., STARKS P.J. and AGAM N., 2008, A thermal-based remote sensing technique for routine mapping of land-surface carbon, water and energy fluxes from field to regional scales, Remote Sensing of Environment, 112, 4227–4241.

BARNOLA J. M., RAYNAUD D., KOROTKEVICH Y. S. and LORIUS C., 1987, Vostok ice core provides 160,000-year record of atmospheric CO2, Nature, 329, 408–414, doi: 10.1038/329408a0, data from ftp://ftp.ncdc.noaa.gov/pub/data/paleo/icecore/ antarctica/vostok/co2.txt.

BARNOLA J.-M., RAYNAUD D., LORIUS C. and BARKOV N.I., 2003, Historical CO_2 record from the Vostok ice core. In Trends: A Compendium of Data on Global Change. Carbon Dioxide Information Analysis Center, Oak Ridge National Laboratory, U.S. Department of Energy, Oak Ridge, Tenn., U.S.A. *Revised February 2003*, data from http://cdiac.esd.ornl.gov/ftp/trends/co2/vostok.icecore.co2, http://cdiac.ornl.gov/trends/co2/vostok.html.

BECK A.E. and JUDGE A., 1969, Analysis of heat flow data – I. Detailed observation in a single borehole, Geophys. J. Res. astr. Soc., 18, 145–158.

BECK A.E., 1982, Precision logging of temperature gradients and the extraction of past climate, Tectonophysics, 83, 1–11.

BELTRAMI H., SMERDON J., POLLACK H. and HUANG S., 2002, Continental heat gain in the global climate system, Geophys. Res. Lett., 29, 8, 10.1029/2001GL014310.

BELTRAMI H., BOURLON E., KELLMAN L. and GONZALEZ-ROUCO J. F., 2006, Spatial patterns of ground heat gain in the Northern Hemisphere, Geophys. Res. Lett., 33, L06717, doi:10.1029/2006GL025676.

BERGER A. and LOUTRE M.F., 1991, Insolation values for the climate of the last 10 million of years, Quaternary Sciences Review, 10, 4, 297–317, data from http://gcmd.nasa.gov/records/GCMD_EARTH_LAND_NGDC_PALEOCLIM_INSOL.html.

BIRCH F., 1948, The effect of pleistocene climatic variations upon geothermal gradient, Am. J. Sci, 61, 567–630.

BLUNIER T., CHAPPELLAZ J., SCHWANDER J., DÄLLENBACH A., STAUFFER B., STOCKER T., RAYNAUD D., JOUZEL J., CLAUSEN H.B., HAMMER C.U. and JOHNSEN S.J., 1998, Asynchrony of Antarctic and Greenland climate change during the last glacial period, Nature, 394, 739–743.

BODRI L. and CERMAK V., 2007, Borehole climatology. A new method on how to reconstruct climate, Elsevier Science, 352 pp.

BODRI L. and CERMAK V., 1997, Reconstruction of remote climate changes from borehole temperatures, Glob. Planet. Change, 1997b, 15, 47–57.

CARSLAW H.S. and JAEGER J.C., 1959, Conduction of Heat in Solids, 2nd ed., Oxford Univ. Press, New York, 510 pp.

CERMAK V., 1971, Underground temperature and inferred climatic temperature of the past millennium, Palaeogeogr. Palaeoclim. Palaeoecol., 10, 1–19.

CHOUDHURY B. J., IDSO S. B. and REGINATO R. J., 1987, Analysis of an empirical model for soil heat flux under a growing wheat crop for estimating evaporation by an infrared-temperature based energy balance equation, Agricultural and Forest Meteorology, 39, 283–297.

DAHL-JENSEN D., MOSEGAARD K., GUNDESTRUP N., CLOW G.D., JOHNSEN S.J., HANSEN A.W. and BALLING N., 1998, Past temperatures directly from the Greenland Ice Sheet, Science, 282, 268–271.

DEMEZHKO D.Yu. and SHCHAPOV V.A., 2001, 80,000 years ground surface temperature history inferred from the temperature-depth log measured in the super deep hole SG-4 (the Urals, Russia), Global Planet. Change, 29 (1–2), 219–230.

DEMEZHKO D.Yu., RYVKIN D.G., OUTKIN V.I., DUCHKOV A.D. and BALOBAEV V.T., 2007, Spatial distribution of Pleistocene/Holocene warming amplitudes in Northern Eurasia inferred from geothermal data, Clim. Past, 3, 559–568.

DEMEZHKO D. Yu. and SOLOMINA O.N., 2009, Ground Surface Temperature Variations on Kunashir Island in the Last 400 Years Inferred from Borehole Temperature Data and Tree-Ring Records, Doklady Earth Sciences, 426, 4, 628–631.

FORSSTRÖM P.-L., 2005, Through a glacial cycle: simulation of the Eurasian ice sheet dynamics during the last glaciation, Annales Academiae Scientiarum Fennicae, Geologica-Geographica, 168, 94 pp.

GLUSHANIN L.V., SHAROV N.V. and SHCHIPTSOV V.V. (eds.), 2011, Palaeoproterozoic Onega structure (Geology, Tectonics, Deep structure and Mineralogeny), KSC., Petrozavodsk, 431 pp. (in Russian).

GOLOVANOVA I.V., SAL'MANOVA R.Yu. and DEMEZHKO D.Yu., 2012, Climate reconstruction in the Urals from geothermal data, Russian Geology and Geophysics, 53, 1366–1373.

HUANG S., 2006, Annual heat budget of the continental landmasses, Geophys. Res. Lett., 33, L04707, 1851–2004, doi:10.1029/2005GL025300.

INDERMUHLE A., MONNIN E., STAUFFER B., STOCKER T.F. and WAHLEN M., 1999, Atmospheric CO2 concentration from 60 to 20 kyr BP from the Taylor Dome ice core, Antarctica, Geophy. Res. Lett., 27, 735–738, data from http://www.ncdc.noaa.gov/paleo/taylor/taylor-glacial.html.

INDERMUHLE A., STOCKER T.F., JOOS F., FISCHER H., SMITH H.J., WAHLEN M., DECK B., MASTROIANNI D., TSCHUMI J., BLUNIER T., MEYER R. and STAUFFER B., 1999b, Holocene carbon-cycle dynamics based on CO2 trapped in ice at Taylor Dome, Antarctica, Nature, 398, 121–126, data from ftp://ftp.ncdc.noaa.gov/pub/data/paleo/icecore/antarctica/taylor/.

KLEMAN J. and HATTESTRAND C., 1999, Frozen-bed Fennoscandian and Laurentide ice sheets during the last glacial maximum, Nature, 402, 63–66.

KRAPEZ J-C., OLIOSOB A. and COUDERTC B., 2009, Comparison of three methods based on the Temperature-NDVI diagram for soil moisture characterization, Proc. of SPIE, 7472, 74720Y, 1–12, doi: 10.1117/12.830451.

KUKKONEN I.T., GOSNOLD W.D. and ŠAFANDA J., 1998, Anomalously low heat flow density in eastern Karelia, baltic Shield: a possible paleoclimate signature, Tectonophysics, 291, 235–249.

KUKKONEN I.T, RATH V., KIVEKAS L., ŠAFANDA J. and ČERMAK V., 2011, Geothermal studies of the Outokumpu Deep Drill Hole, Finland: Vertical variation in heat flow and palaeoclimatic implications, Physics of the Earth and Planetary Interiors, 188, 9–25.

LACHENBRUCH A.H. and MARSHALL B.V., 1986, Changing climate: Geothermal evidence from permafrost in the Alaskan Arctic, Science, 234, 689–696.

LUNKKA J. P., SAARNISTO M., GEY V. P., DEMIDOV I. and KISELOVA V., 2001, Extent and age of the Last Glacial maximum in the southeastern sector of the Scandinavian Ice Sheets, Global Planet. Change, 31, 407–426.

MAJOROWICZ, J., 2012, Permafrost at the ice base of recent Pleistocene glaciations – inferences from borehole temperature profiles, Bulletin of Geography-Physical Geography Series, V.5(1), 7-28, DOI: 10.2478/v10250-012-0001-x

MAJOROWICZ J., SKINNER W. and SAFANDA J., 2012a, Western Canadian Sedimentary Basin temperature–depth transients from repeated well logs: evidence of recent decade subsurface heat gain due to climatic warming, J. Geophys. Eng., 9, 127–137, doi:10.1088/1742-2132/9/2/127.

MAJOROWICZ J., SAFANDA J., and OSADETZ K., 2012b, Inferred gas hydrate and permafrost stability history models linked to climate change in the Beaufort-Mackenzie Basin, Arctic Canada. Clim. Past, 8(2), 667–682.

NARKISOVA V.V. (ed.), 2009, The Onega parametric borehole, Report, Yaroslavl (in Russian), http://karelnedra.karelia.ru/geolinform/onego_skv_0.htm.

PEDRO J.B., RASMUSSEN S.O. and VAN OMMEN T.D., 2012, Tightened constraints on the time-lag between Antarctic temperature and CO2 during the last deglaciation, Clim. Past, 8, 1213–1221, doi:10.5194/cp-8-1213-2012, www.clim-past.net/8/1213/2012/.

RAJVER D., SAFANDA J. and SHEN P.Y., 1998, The climate record inverted from borehole temperatures in Slovenia, Tectonophysics, 291, 263–276.

SAARNISTO M. and SAARINEN T., 2001, Deglaciation chronology of the Scandinavian Ice Sheet from the Lake Onega Basin to the Salpausselka End Moraines, Global Planet. Change, 31, 387–405.

SAFANDA J., SZEWCZYK J. and MAJOROWICZ J., 2004, Geothermal evidence of very low glacial temperatures on a rim of the Fennoscandian ice sheet, Geophys. Res. Lett., 31, L07211, doi:10.1029/2004GL019547.

SHAKUN J.D., CLARK P.U., HE F., MARCOTT S.A., MIX A.C., LIU Z., OTTO-BLIESNER B., SCHMITTNER A. and BARD E., 2012, Global warming preceded by increasing carbon dioxide concentrations during the last deglaciation, Nature, 4, 484(7392):49-54, doi: 10.1038/nature10915.

SMITH H. J., FISCHER H., MASTROIANNI D., DECK B. and WAHLEN M., 1999, Dual modes of the carbon cycle since the Last Glacial Maximum, Nature, 400, 248–250, data from ftp://ftp.ncdc.noaa.gov/pub/data/paleo/icecore/antarctica/taylor/.

SONIN G.V., 2001, Thermophysical properties of soils and neutral layer temperatures in the CIS territory, Georesources, 1(5), 16–19 (in Russian).

WANG J. and BRAS R.L., 1999, Ground heat flux estimated from surface soil temperature, J. Hydrology, 216, 3–4, 214–226.

YLI-HALLA M. and MOKMA D.L., 1998, Soil temperature regimes in Finland, Agriculture and Food Science in Finland, 7, 507–512.